

Design, Construction, and Experimental Testing of a Parabolic Trough Collector for Process Heat Applications

Husni T. Izweik¹, Ahmed M. Ahmed^{2,3}, Abdelhafeed A. Albusefi³

Lecturer, Dept. of Mechanical Engineering, Sabratha Engineering College, Sabratha University, Libya¹

Assistant Professor, Dept. of Mechanical Engineering, Faculty of Engineering Science, Nyala University, Sudan²

Assistant Professor, Dept. of Mechanical Engineering, Sabratha Engineering College, Sabratha University, Libya³

ABSTRACT: One of the most important applications of the solar energy is the Parabolic Trough Collector. During last decades until now; there are several promising developments in the field of the Parabolic Trough Collectors and their applications. In this research paper design, construction and testing of two Parabolic Trough Collectors fabricated from the available local materials has been experimentally investigated under local climate conditions of Sabratha City in Libya (latitude 32.8° N, longitude 12.5°E). Water is chosen as the heat transfer fluid, and the testing period taken from 30th of December 2015 to 5th of April 2016. The testing results showed that the maximum instantaneous thermal efficiency reached 52.7% for a direct solar radiation of 243 W/m² at a flow rate of 0.24 L/min at 10:00 AM on 4th of January 2016. Moreover, a maximum outlet temperature reached 88.1 °C for a direct solar radiation of 944 W/m² at a flow rate of 0.24 L/min at 1:00 PM on 30 March 2016. Based on these results, Libya holds a real potential for the PTC technology to meet the increasing demand for water heating systems.

KEYWORDS: Parabolic Trough Collector, water outlet temperature, collector thermal Efficiency, Collector Design.

I. INTRODUCTION

Parabolic Trough Collectors (PTC) are devices use metal sheet mirrors or aluminum foil sheets in the shape of parabolic shapes to reflect and concentrate sun radiations towards a receiver tube located at the focus of the parabolic cylinder. The receiver absorbs the solar radiation and transforms it into thermal energy which was transported by a fluid medium flowing through the receiver tube. This method of concentrated solar collection has the advantage of high efficiency and low cost. Therefore, PTC is the leading technology for large scale exploitation of solar energy, and currently became the most proven solar thermal technology for a solar steam generation.

Libya is one of the biggest countries in Africa with an area about 1,760,000 km², lies between latitudes 19° and 34°N, and longitudes 9° and 26°E. The total average of global solar irradiance on the horizontal surface ranges between 1600 - 2300 kWh/m²[1], [2]. These values correspond to average daily range between 5 and 7 kWh/m².day, Thus, it owns a great potential of solar energy. Recent studies have shown that the significance of renewable energy resources represents the best alternative to traditional fossil fuel in Libya [3]. The demand of energy for water heating and air-conditioning is one of the main areas for energy consumption which is proportional to the availability of solar radiation during the day. Introducing renewable energies on the housing and industrial sectors should lead to energy savings. Therefore, solar thermal systems became one of the most attractive solutions for these problems.

The application of PTCs can be divided into two main groups[4]: the first group is the industrial processes that need temperature ranging from 100°C to 250°C in their processes like space heating, cooling, drying, and refrigeration. The second group is the parabolic trough solar power generation that requires temperatures ranging from 300°C to 400°C which is the main application of the concentrated solar power technology. The PTC has been designed and studied analytically and experimentally by many investigators several decades ago. In his paper, Treadwell considered

International Journal of Innovative Research in Science, Engineering and Technology

(An ISO 3297: 2007 Certified Organization)

Vol. 5, Issue 9, September 2016

how optical and thermal effects influence the efficiency of a PTC [5]. He found that rim angles of 90 minimized the maximum distance between the parabolic reflector and the focus. Since the receiver diameter is proportional to this distance, thermal losses, which are proportional to the diameter itself, are reduced. Clark studied the principle design factors that influence the performance of a PTC[6]. Factors like spectral directional reflectivity of the mirror, the mirror-receiver tube intercept factor, the end loss, the incident angle modifier, receiver tube misalignment, and effect of tracking errors are considered for this analysis. Kalogirou et al. presented a PTC design with high stiffness-to-weight ratio and a low-labor manufacturing process[7]. The structure was made of polyester resin and woven fiberglass cloth, with plastic conduits that provide reinforcement. Valan Arasu and Sornakumar presented a simple, low-cost hand lay-up method for manufacturing PTC [8] based on the previous work of Kalogirou et al. [7]. The design proposed consists of a smooth 90 rim angle, reinforced parabolic trough made of layers of polyester resin and chopped strand fiberglass. In a paper published in the same year [9], the authors outlined a design optimization method based on three parameters: the collector aperture, the rim angle, and the receiver diameter. They also proposed a tracking mechanism with a control system consisting of three light dependent resistors. A torque box structure was also used by Brooks et al. with a mix of advanced and less sophisticated technologies to manufacture a reflector made of stainless steel sheets covered with the aluminium film[10]. This solution grants accessibility, accuracy, ease of fabrication, and cost reduction. The authors also reported that the instantaneous thermal efficiency for a low-temperature PTC that uses a glass cover does not translate into a significant increase in the efficiency of temperatures near 100 °C. P. Bendt et al.[11] reported an excellent application of the PTC for line-focus solar concentrators in a Solar Energy Research Institute (SERI).

Venegas-Reyes et al. described a light but robust structure of aluminum made only using hand tools designed for low-enthalpy steam generation and hot water[12]. This PTC has a rim angle of 45° and the receiver without a glass cover to reduce costs. In another work published in 2013 [13], the authors presented five PTCs for the same purpose; three of them have a rim angle of 90° and the other two have a rim angle of 45°. In the construction and assembly of both collectors, only hand tools are required. The design of both collectors considers unshielded receivers and without glass cover to reduce manufacturing and transportation costs. They carried out thermal and optical analyses for each collector, and the results showed the peak efficiency of 35% and 67% for the PTC with a rim angle of 45° and 90° respectively. Recently, Gianluca Coccia et al.[14] presented a prototype of a PTC with a 90 rim angle and a concentration ratio of 9.25 built from fiberglass and extruded polystyrene, called UNIVPM.01, with a tracking system based on a solar position computer program. The main features of their prototype are its cost-effectiveness, low weight, high mechanical resistance, and ease of manufacture. The thermal efficiency of a PTC is derived and found to be in the form of a linear equation with intercept is 0.658, and the slope is 0.683 which is comparable to other similar collectors available in the literature. Ahmed M. Ahmed et al. [15] run an experimental evaluation of a PTC under Libyan climate in the winter season. They used water as heat transfer fluid. Their experimental results showed that the maximum instantaneous thermal efficiency reached 43.9% for a direct solar radiation of 474 W/m² at a flow rate of 14.4kg/hr, and the maximum outlet temperature reached 79.5 °C for a direct solar radiation of 650W/m² at a flow rate of 14.4kg/hr. They stated that Libya holds a real potential for the PTC technology to meet the increasing demand for water heating.

The first objective of this paper is to design, construct, and test a PTC fabricated at the Sabratha Engineering College at Sabratha University. The secondary objectives are to produce medium water temperature for residential and industrial processes.

II. PTC DESIGN

A prototype PTC is made from available local materials. The collector is designed with simple parabolic equations. A cross section of a PTC is shown in Fig. 1. where various important factors are shown. The incident radiation on the PTC at the rim of the collector (where the mirror radius, r_r is maximum) makes an angle, ϕ_r with the center line of the collector, which is called the rim angle. From geometrical relations of the parabolic section, the equation of the parabola in terms of the coordinate system is given as:

$$x^2 = 4fy \quad (1)$$

By substituting $y = h$ regarding the focal length and aperture diameter is $x = a/2$:

$$h = a^2 / (16f) \quad (2)$$

International Journal of Innovative Research in Science, Engineering and Technology

(An ISO 3297: 2007 Certified Organization)

Vol. 5, Issue 9, September 2016

For a parabolic reflector, the radius, r , shown in Fig. 1. is given by:

$$r = \frac{2f}{1 + \cos(\varphi)} \tag{3}$$

Where φ is the angle between the reflected beam and the collector axis at the focus. As φ varies from 0 to φ_r , r increases from f to r_r , therefore, equation (3) become

$$r_r = \frac{2f}{1 + \cos(\varphi_r)} \tag{4}$$

Another parameter related to the rim angle is the aperture of the parabola, (a). From Fig. 1. and simple trigonometry, it can be found that:

$$a = 2 r_r \sin(\varphi_r) \tag{5}$$

By substituting equation (4) into equation (5) gives the following:

$$a = \frac{4f \sin(\varphi_r)}{1 + \cos(\varphi_r)} \tag{6}$$

$$\tan\left(\frac{\varphi_r}{2}\right) = \frac{a}{4f} \tag{7}$$

The Geometrical concentration ratio C is the ratio of the aperture area A_a , to the receiver surface area A_{rec}

$$C = \frac{A_a}{A_{rec}} = \frac{a}{\pi D_o} \tag{8}$$

The curve length (S) of the reflective surface is given by: [22]

$$S = \frac{H}{2} \left[\sec\left(\frac{\varphi_r}{2}\right) \cdot \tan\left(\frac{\varphi_r}{2}\right) + \ln\left(\sec\left(\frac{\varphi_r}{2}\right) + \tan\left(\frac{\varphi_r}{2}\right)\right) \right] \tag{9}$$

Where H is the latus rectum of the parabola which is calculated by:

$$H_p = 4f \tan(\varphi_r / 2) \tag{10}$$

For the same aperture width, various rim angles are possible as shown in Fig. 2. It is also shown that, for different rim angles, the focus-to-aperture ratio, which defines the curvature of the PTC changes. It can be announced that, with a rim angle 90° , the mean focus-to-reflector distance is minimized. The collector surface area decreases as the rim angle is decreased. There is thus a temptation to use smaller rim angles because the sacrifice in optical efficiency is small, but the saving in reflective material cost is great[16].

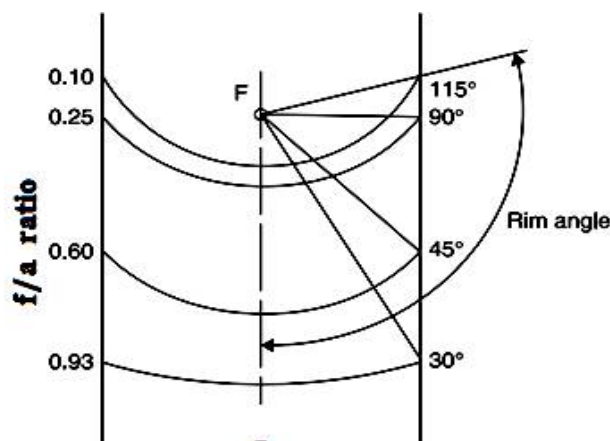


Fig. 1: Parabola focal length and curvature

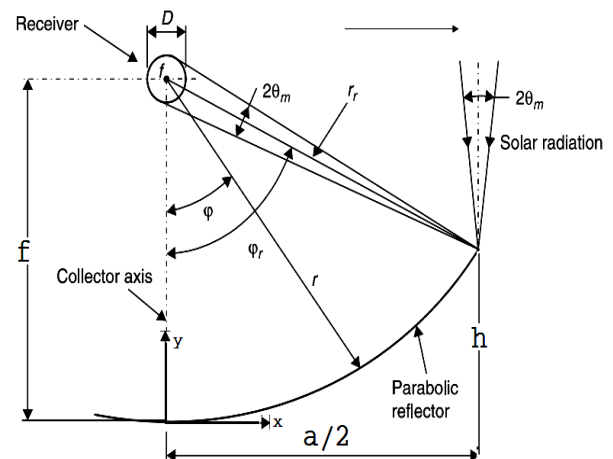


Fig. 2: Cross-section of the PTC with circular receiver

International Journal of Innovative Research in Science, Engineering and Technology

(An ISO 3297: 2007 Certified Organization)

Vol. 5, Issue 9, September 2016

III. PTC CONSTRUCTION

The construction and assembly of the PTC are done at the workshop of the mechanical engineering department at Sabratha Engineering College at Sabratha University. The body of the first PTC is made of 10 pieces of plywood traded in parabolic shapes as shown in fig.3(a), fixed in equal spaces by 4 solid steel rods and wooden plates 3 m length at both length sides as shown in fig.3(b). This assembly allows the PTC to be adjusted and varying its slope through a manual tracking process. The reflecting surface is made of Formica sheet 2.8 m length and 1.04 m width which gives an effective aperture area of 2.912 m² coated by a bright aluminum foil with a reflectivity value ($\rho = 0.85$) as shown in fig.3 (c). The second PTC is made from thin steel sheet 2.0 mm thickness, 2.0m length and 1.04 m width coated by a bright aluminum foil with the same properties as first PTC. The reflecting surface aperture effective area is 2.08m². The whole arrangements are fitted on a steel frame consists of two mechanical assemblies: stationary base assembly and moving assembly as shown in Fig.3 (d). The two assemblies have the same optical characteristics. Therefore, they are arranged in series as illustrated in fig. 4, and their receivers are connected by a flexible tube to give a total length of 4.8m.

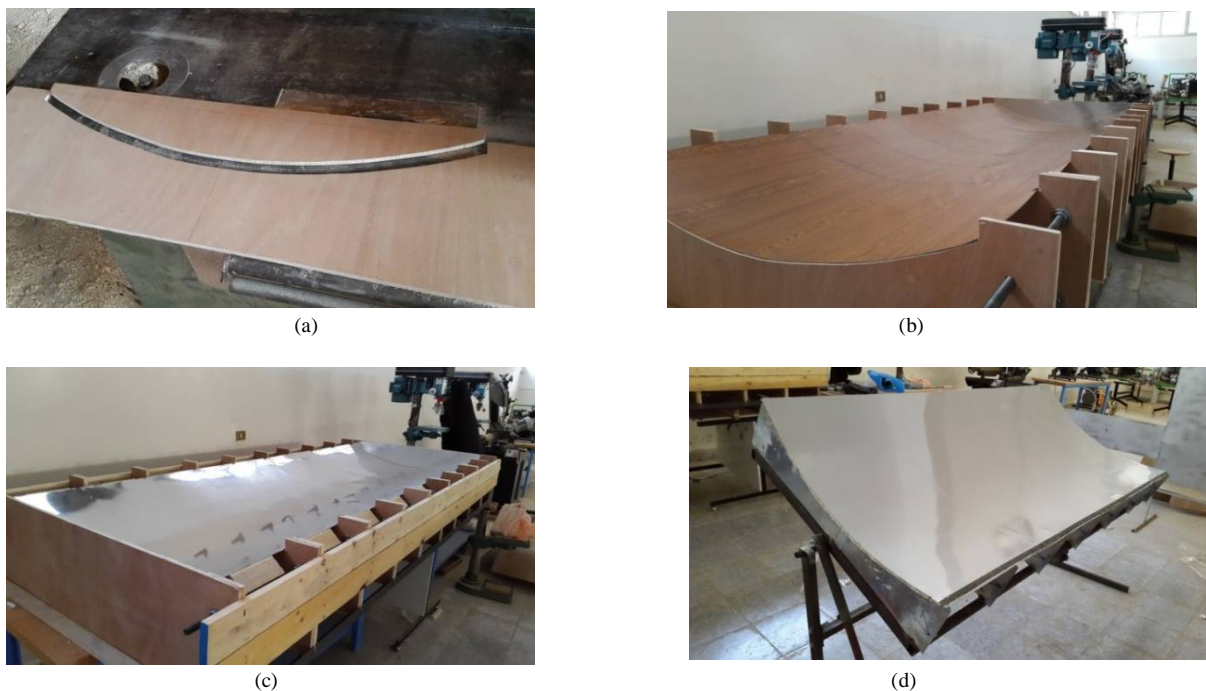


Fig. 3. : PTC Construction (a) Tracing the parabolic shape, (b) Fixing the parabolic surface
(c) Coating the parabolic surface with reflector, (d) Steel frame parabolic collector.

A mild steel tube was selected from the available local tubes to serve as a receiver with an internal diameter ($D_i = 0.017m$), external diameter ($D_o = 0.021m$), absorptivity, emissivity ($\epsilon_{rec} = 0.9$) and thermal conductivity ($k_{rec} = 80W/m \cdot ^\circ C$). It is acceptable according to the aperture width to give geometrical concentration ratio of 15.763. The receiver used in this study is chosen to be without glass cover. In fact, the overall heat loss coefficient could be improved by using a glass-shielded receiver. However, considering the temperature range for heating water purposes between 70 and 110 °C, it is possible to consider that adding a glass-shielded tube is not necessary because its fabrication in developing countries like Libya is difficult, and must be imported from abroad. The receiver tube was painted with black paint, insulated from its upper area and fixed at the reflector focal length, to receive the solar radiation from the reflector.

International Journal of Innovative Research in Science, Engineering and Technology

(An ISO 3297: 2007 Certified Organization)

Vol. 5, Issue 9, September 2016



Fig. 4: Final setup of the experimental work

The ratio of focal length to aperture was selected from fig. 2. to be $(f/a)=0.5$ then the rim angle ϕ_r was calculated from equation (7), the rim radius (r_r) from equation (4). The aperture width (a) from equation (5), the parabola latus rectum (H) from equation (10). The curve length of the parabola (S) from equation (9) and geometrical concentration ratio C was calculated from equation (8). The characteristics of the designed model have the following values as given in Table 1.

Table1: Geometrical Characteristics of the PTC model

Characteristic	Symbol	Value
Aperture width (m)	a	1.0
Aperture area (m ²)	A_a	4.992
Collector height(m)	h	0.125
Collector Length(m)	L	4.8
Focal length(m)	f	0.5
Geometrical concentration ratio	C	15.76
Parabola curve length(m)	S	1.04
Parabola latus rectum(m)	H	1.0
Receiver area (m ²)	A_{rec}	0.3167
Receiver inner diameter(m)	D_i	0.017
Receiver outer diameter(m)	D_o	0.021
Rim angle(⁰)	ϕ_r	53.13
Rim radius(m)	r_r	0.625

IV. EXPERIMENTAL SETUP AND PROCEDURE

A photographic view of the PTC used in the experimental investigation is shown in Fig.4. The experimental work is done in an open flow from 30th of December 2015 to 5th of April 2016. The test rig is placed in an open space, and the readings are taken from 10:00 AM to 2:00 PM daily. The system consists of the constructed collector, 1m³ storage tank and measuring instruments. The storage tank is used for storing the cold water, it was made of iron sheet

International Journal of Innovative Research in Science, Engineering and Technology

(An ISO 3297: 2007 Certified Organization)

Vol. 5, Issue 9, September 2016

and fixed at 3m above the collector level so that the water flow due to the gravity. A flexible pipe made of plastic is used for carrying the cold water from the storage tank to the receiver. A control valve is connected to the storage tank for controlling the mass flow rate. The flowmeter was connected before the inlet of the receiver tube to measure the water flow rate. During the experiment, many measurements are taken at a time interval of 15 minutes. The temperature of water inlet (T_{in}), water outlet (T_{ou}), ambient (T_a) and tube surface temperature (T_s) are measured using digital thermometers. Air velocity (V) was measured using a digital anemometer. Water flow rate (m^0) was measured using flowmeter, and the solar radiation intensity (I) was measured using digital pyrheliometer. The specifications of the measuring devices used during the experiment are shown in Table 2.

Table 2 Measuring instruments specifications

Device	Type	Fluid	Operating range	Accuracy
Thermometer	Tastotherm MP2000	Water	Temperature: (-200–1300) °C	± 2 °C
Anemometer	GM8901-2-#7183	Air	Temperature: (0– 45) °C Velocity : (0–45) m/s	± 2 °C ± 3 %
Flowmeter	MPB	Water	Flow rate : (0–50) g/s	± 2 %
Pyrheliometer	METEON CMP6	Solar radiation	Irradiance: (0 – 2000) w/m ²	16.34x10 ⁻⁶ v/w/m ²

V. SYSTEM PERFORMANCE CALCULATIONS

Thermal performance of PTC was evaluated using the measured temperatures of heat transfer fluid (HTF) for inlet and outlet, mass flow rate, ambient temperature, wind speed, and solar radiation intensity.

The useful heat gain is the instantaneous heat energy gained by the HTF during its flow between the inlet and outlet of the receiver. It is calculated from the flowing equation:

$$Q_u = m^0 C_p (T_{ou} - T_{in}) \tag{11}$$

Where (T_{in}) and (T_{ou}) denote the temperature of the HTF at the inlet and outlet of the receiver measured at the same time, (C_p) is specific heat of the water in ($J/(kg.K)$), and (m^0) is the mass flow rate of the HTF measured in (g/s)

The thermal efficiency of the PTC is defined as the ratio of the instantaneous useful heat gained by the HTF, and the instantaneous solar beam radiation incident (I) on the given aperture area of the collector (A_a). The instantaneous thermal efficiency (η_{th}) is calculated as follows:

$$\eta_{th} = \frac{m^0 C_p (T_{ou} - T_{in})}{I.A_a} = \frac{Q_u}{I.A_a} \tag{12}$$

VI. RESULTS AND DISCUSSION

Data of inlet and outlet temperatures along with thermal efficiency calculated from equation (12) and heat gained calculated from equation (11) are plotted and demonstrated in detail in the following figures:

Fig. 5. shows variations of the solar radiation measured for two selected days, one is at Autumn season specifically on 26th of January, and the other day is at the beginning of the Spring season specifically on 29th of March 2016. The measured radiation rates are taken from 10:00 AM to 4:00 PM. At 10:00 AM, the solar intensity is low. As the time passes, the intensity starts to rise until reaching the peak around 1:30 PM. After that time, the intensity decreases till the end of the experiment. It can be noticed that the solar the value of the radiation increases as the time was closer to spring, this is due to the increased elevation angle of the sun, where the earth is closer to the sun.

International Journal of Innovative Research in Science, Engineering and Technology

(An ISO 3297: 2007 Certified Organization)

Vol. 5, Issue 9, September 2016

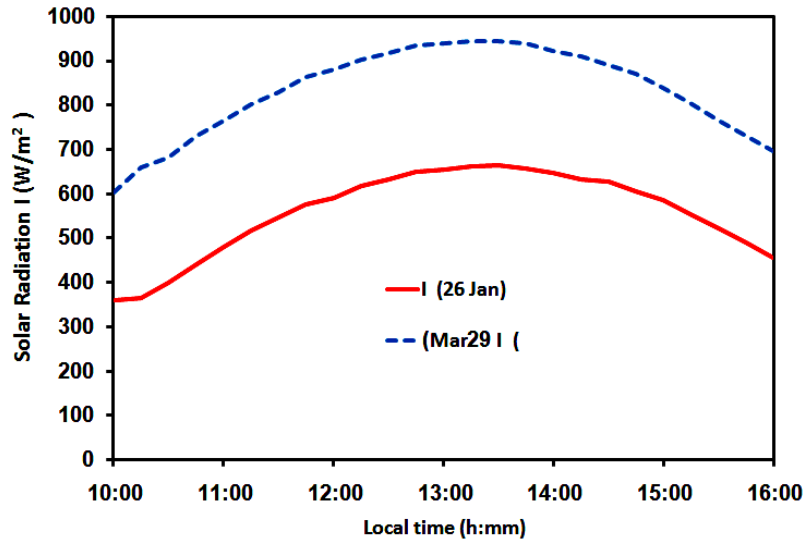


Fig. 5: Variation of solar radiation (I) on 26th January and 29th March with time

Fig. 6. shows variations of the useful heat gain calculated from equation (11) for the test days of 26th of January and 29th of March. At 10:00 AM, the gained heat is low due to the low rate of solar radiation, then as time passes, it starts to increase until reaching the peak around 12:00 to 1:30 PM which indicates that the solar radiation rate influences the energy collected. After 2:00 PM, the useful heat gain decreases until the end of the experiment as a result of the decreased solar intensity.

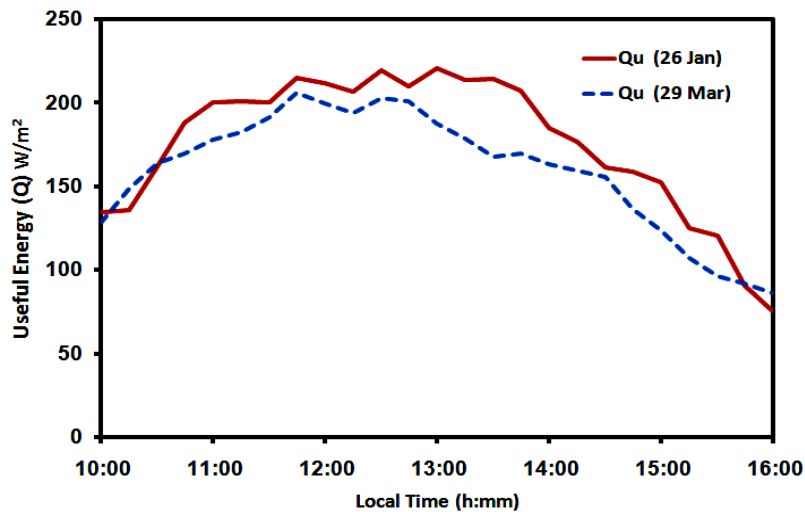


Fig. 6: Variation of useful heat gained (Q_u) on 26th January and 29th March with time

Fig. 7. shows the instantaneous thermal efficiency during the experiment period for the two days. It is noticed that the efficiency is high at the beginning of the experiment because the solar radiation is lower (equation (12)). Maximum values of the thermal efficiency for these days are 42.7% and 24.1% on 26th of January and 29th of March respectively. As time passes; the efficiency starts to decrease until it reaches its minimum values at the end of the experiment because the thermal efficiency is inversely proportional to the solar radiation intensity. It is noticed that the

International Journal of Innovative Research in Science, Engineering and Technology

(An ISO 3297: 2007 Certified Organization)

Vol. 5, Issue 9, September 2016

thermal efficiency on 26th of January is higher 29th of March, the reason is that the solar radiation intensity in January is lower than March, and the thermal losses in March higher than in January.

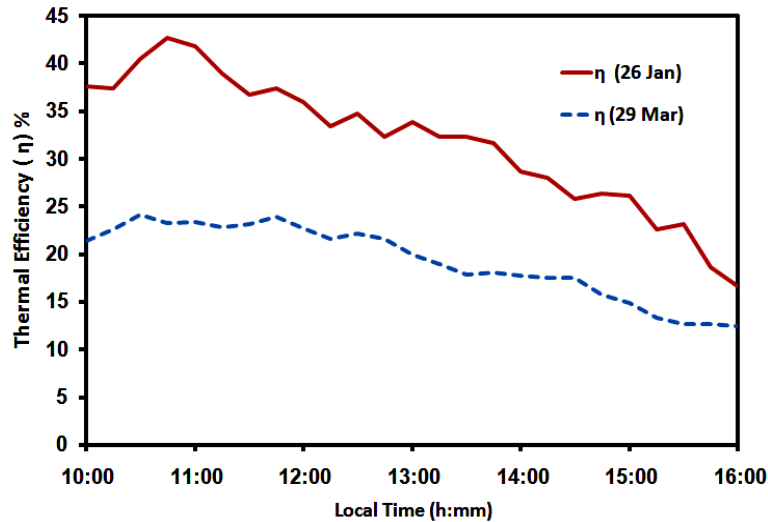


Fig. 7: Variation of instantaneous thermal efficiency (η) on 26th January and 29th March with time

Fig. 8. shows the variation of ambient temperature and wind speed with time. At the beginning of the test, the ambient temperature is low with values around 10 °C to 17.6 °C. It starts to increase as the radiation intensity increases until it reaches maximum values around 18 °C to 20 °C from 2:30 PM to 3:30 PM. Then, it decreases slightly at the end of the test. The minimum wind speed is found with a value of 0.1 m/s and the maximum has a value 1.7 m/s, and between these values, it is fluctuating up and down until the end of the test according to the local weather condition.

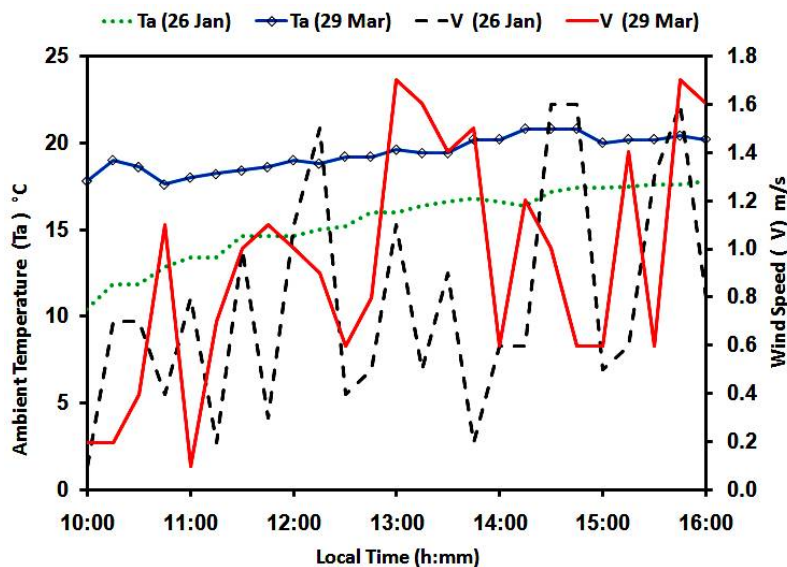


Fig. 8: Variation of ambient temperature (T_a) and wind speed (V) on 26th January and 29th March with time

Fig. 9. shows the variation of the solar radiation with experiment days between 10:00 AM, and 2:00 PM. It can be observed that the solar radiation increases gradually from the beginning of the experiments in January till April the

International Journal of Innovative Research in Science, Engineering and Technology

(An ISO 3297: 2007 Certified Organization)

Vol. 5, Issue 9, September 2016

end time of the experimental work. The reason is due increasing the sun elevation angle as the Earth approaching the Sun at this period of the year, as a result of the movement of the Sun from the Tropic of Capricorn in the south to the Tropic of Cancer in the north. There are some discrepancies of the solar radiation in a few days due to the presence of fogs and rain in these days. The maximum value of the solar radiation is 944 W/m^2 at 1:00 PM on 30th of March 2016.

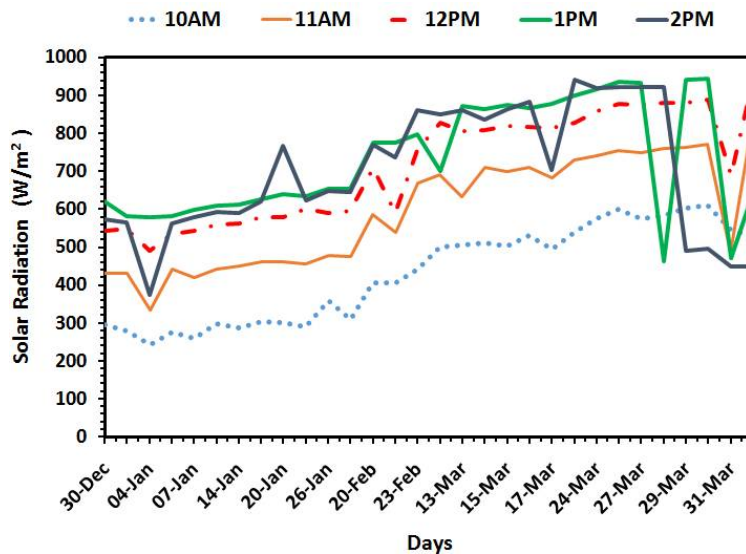


Fig. 9: Variation of solar radiation during the experiment days

Fig. 10. shows the variation of the outlet water temperature with experimental days between 10:00 AM, and 2:00 PM. It can be noticed that the outlet water temperature starts to increase each day from the beginning of the experiment at 10:00 AM to reach its maximum value at 1:00 PM then, it starts to decrease. This variation is same to the solar radiation behavior because the outlet water temperature depends mainly on the solar radiation intensity.

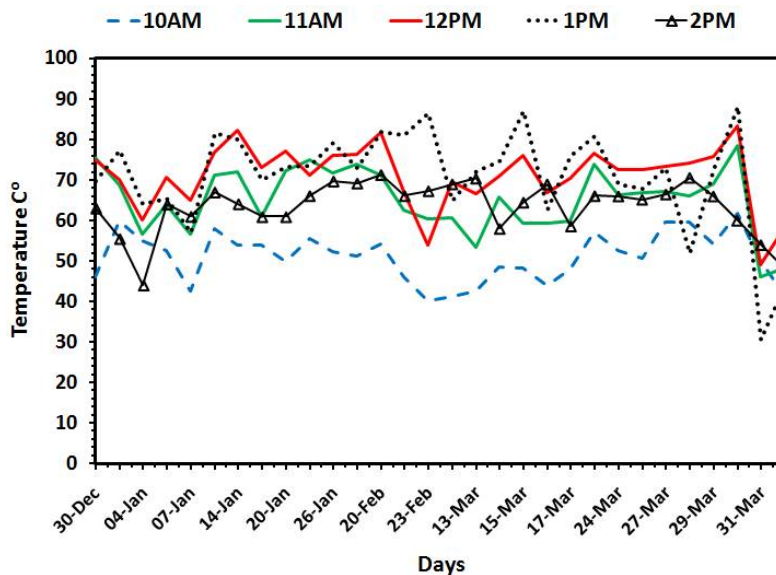


Fig. 10: Variation of outlet temperature at different times during the experiment days

International Journal of Innovative Research in Science, Engineering and Technology

(An ISO 3297: 2007 Certified Organization)

Vol. 5, Issue 9, September 2016

The maximum outlet temperature obtained during the experimental work is 88.1 °C on 30th of March 2016 at 1:00 PM. This temperature is suitable for residential and industrial uses. There are some fluctuations of the outlet water temperature in some days due to the presence of fogs and rain in these days. The outlet water temperature is expected to reach more than 100 °C in summer when the solar radiation reaches its maximum values.

Fig. 11. shows the variation of the thermal efficiency with experimental days between 10:00 AM, and 2:00 PM. It can be obviously observed that the thermal efficiency is high at January when the solar radiation rates are low, and it decreases until it reaches its lowest values at the end of the experimental days at the beginning of April when the solar radiation rates are high. It can also be seen that the thermal efficiency is higher at the beginning of the experimental day at 10:00 AM and starts to decrease gradually to reach its minimum value at the end of the experimental day at 4:00 PM. The reason is that thermal efficiency is inversely proportional to the solar radiation intensity (equation 12).

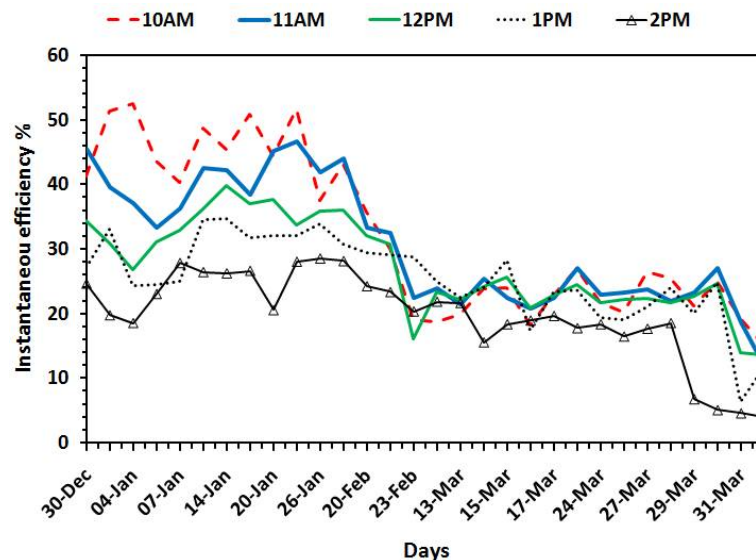


Fig. 11: Variation of efficiency at different times during the experiment days

VII. CONCLUSIONS

Design, construction, and experimental study were presented to evaluate the performance of a PTC under Sabratha city in Libya. The experiments are taken from 30th of December 2015 to 5th of April 2016. The collector thermal efficiency and useful heat gained curves showed a similar behavior with the data published by other researchers. From these results, the maximum value of the thermal efficiency for the test period is 52.5 %, and the maximum value of the outlet water temperature is found to be 88.1°C. Because it is the first attempt to manufacture such collector locally, the obtained characteristic curves of the tested collector are considerably lower than that of a typical collector made by professional companies. This is attributed to the higher thermal losses caused by the absence of the evacuated glass envelope around the absorber tube, the end losses of the collector, and the inaccuracy of the tracking system. The following conclusions could be drawn:

- Libya climate is suitable for application of the PTC in the area of water heating purposes for residential and industrial uses.
- It is recommended to use a receiver with evacuated glass envelope to improve the thermal efficiency and reduce the thermal losses of the PTC.
- It is recommended to use an automatic tracking system to reduce the end losses of the collector, and hence improve the thermal efficiency of the PTC.

International Journal of Innovative Research in Science, Engineering and Technology

(An ISO 3297: 2007 Certified Organization)

Vol. 5, Issue 9, September 2016

ACKNOWLEDGEMENTS

The authors gratefully acknowledge the technical support given for this work by the graduate studies department, Faculty of Engineering, Sabratha University. We also thank the final year students, Taha Algoul and Mohamed Kareem for their support during the experimental work. Finally, we thank the authors of the references cited in this paper that helped in the improvement of quality.

REFERENCES

- [1] F. Ahwide, A. Spena, and A. El-Kafrawy, "Correlation for the Average Daily Diffuse Fraction with Clearness Index and Estimation of Beam Solar Radiation and Possible Sunshine Hours Fraction in Sabha, Ghdames and Tripoli - Libya," *APCBEE Procedia*, vol. 5, pp. 208–220, 2013.
- [2] F. K. Bannani, T. A. Sharif, and A. O. R. Ben-Khalifa, "Estimation of monthly average solar radiation in Libya," *Theoretical and Applied Climatology*, vol. 83, no. 1–4, pp. 211–215, 2006.
- [3] A. M. A. Mohamed, A. Al-Habaibeh, and H. Abdo, "An investigation into the current utilization and prospective of renewable energy resources and technologies in Libya," *Renew. Energy*, vol. 50, pp. 732–740, 2013.
- [4] G. Kumaresan, R. Sridhar, and R. Velraj, "Performance studies of a solar parabolic trough collector with a thermal energy storage system," *Energy*, vol. 47, no. 1, pp. 395–402, 2012.
- [5] G. W. Treadwell, "Design Considerations For Parabolic- Cylindrical Solar Collectors," Albuquerque, New Mexico 87115, 1976.
- [6] J. A. Clark, "An analysis of the technical and economic performance of a parabolic trough concentrator for solar industrial process heat application," *Int. J. Heat Mass Transf.*, vol. 25, no. 9, pp. 1427–1438, 1982.
- [7] S. Kalogirou, P. Eleftheriou, S. Lloyd, and J. Ward, "Low-cost high accuracy parabolic troughs construction and evaluation," *Renew. Energy*, vol. 5, no. 1–4, pp. 384–386, 1994.
- [8] A. Valan Arasu and T. Sornakumar, "Design, manufacture and testing of fiberglass reinforced parabola trough for parabolic trough solar collectors," *Sol. Energy*, vol. 81, no. 10, pp. 1273–1279, 2007.
- [9] S. A. Kalogirou, S. Lloyd, J. Ward, and P. Eleftheriou, "Design and performance characteristics of a parabolic-trough solar collector system," *Appl. Energy*, vol. 47, no. 4, pp. 341–354, 1994.
- [10] M. Brooks, I. Mills, and T. Harms, "Design, construction and testing of a parabolic trough solar collector for a developing-country application," in *proceedings of the ISES Solar World Congress, Orlando, FL, 2005*.
- [11] P. Bendt, A. Rabl, H. W. Gaul, and K. A. Reed, "Optical Analysis and Optimization of Line Focus Solar Collectors," *Solid. State. Electron.*, vol. 41, no. 11, pp. 1787–1793, 1997.
- [12] E. Venegas-Reyes, O. a. Jaramillo, R. Castrejón-García, J. O. Aguilar, and F. Sosa-Montemayor, "Design, construction, and testing of a parabolic trough solar concentrator for hot water and low enthalpy steam generation," *J. Renew. Sustain. Energy*, vol. 4, no. 5, pp. 053103–1 – 053103–18, 2012.
- [13] O. A. Jaramillo, E. Venegas-Reyes, J. O. Aguilar, R. Castrejón-García, and F. Sosa-Montemayor, "Parabolic trough concentrators for low enthalpy processes," *Renew. Energy*, vol. 60, pp. 529–539, 2013.
- [14] G. Coccia, G. Di Nicola, and M. Sotte, "Design, manufacture, and test of a prototype for a parabolic trough collector for industrial process heat," *Renew. Energy*, vol. 74, pp. 727–736, 2014.
- [15] M. A. Ahmed, A. A. Albusefi, and H. T. Izweik, "Experimental Evaluation of a Solar Parabolic Trough Collector under Libyan climate," *Int. J. Eng. Trends Technol.*, vol. 38, no. 1, pp. 32–37, 2016.
- [16] H. P. Garg and J. Prakash, *Solar Energy: Fundamentals and Applications*. Tata McGraw-Hill, 2005.